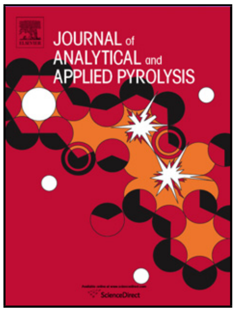

Title: STUDY OF VARIABLES IN ENERGY
DENSIFICATION OF OLIVE STONE BY
HYDROTHERMAL CARBONIZATION

Author: A. Álvarez- Murillo S. Román B. Ledesma E. Sabio

PII: S0165-2370(15)00048-0
DOI: http://dx.doi.org/doi:10.1016/j.jaap.2015.01.031
Reference: JAAP 3414

To appear in: *J. Anal. Appl. Pyrolysis*

Received date: 30-7-2014
Revised date: 12-1-2015
Accepted date: 31-1-2015

Please cite this article as: A.Álvarez- Murillo, S.Román, B.Ledesma, E.Sabio, STUDY OF VARIABLES IN ENERGY DENSIFICATION OF OLIVE STONE BY HYDROTHERMAL CARBONIZATION, Journal of Analytical and Applied Pyrolysis http://dx.doi.org/10.1016/j.jaap.2015.01.031

This is a PDF file of an unedited manuscript that has been accepted for publication. As a service to our customers we are providing this early version of the manuscript. The manuscript will undergo copyediting, typesetting, and review of the resulting proof before it is published in its final form. Please note that during the production process errors may be discovered which could affect the content, and all legal disclaimers that apply to the journal pertain.

STUDY OF VARIABLES IN ENERGY DENSIFICATION OF OLIVE STONE BY HYDROTHERMAL CARBONIZATION

A. Álvarez-Murillo*, S. Román, B. Ledesma, E. Sabio

Departamento de Física Aplicada, Escuela de Ingenierías Industriales, Universidad de Extremadura. Avda. Elvas s/n, 06006 – Badajoz, Spain
*Tel. 0034 924289600, Fax: 0034 924289601, *e-mail:* andalvarez@unex.es

ABSTRACT

The influence of the variables biomass/water ratio (1.1-12.3%), temperature (150 - 250 °C) and residence time (3.2 - 36.8 h) on the hydrothermal carbonization of olive stone has been studied. The implementation of a Design of Experiments – Response Surface Methodology approach allowed the process to be optimized in terms of reactivity (solid yield) and energy densification (increase in higher heating value), and the importance of each variable in the process to be identified. Solid yield ranged between 30.95% and 55.75% and HHV from 22.2 to 29.59 MJ kg^{-1}. Interactions between the different variables involved were investigated to provide more precise control of the overall process so as to satisfy any given energy densification requirement of the final hydrochar.

Keywords: Biofuel, Hydrothermal carbonization, Olive stone, Surface response methods.

Abbreviations list:

Biomass/water ratio: R

Biomass/water ratio-Residence time: R-t

Biomass/water ratio-Temperature: R-T

Central Composite Design: CCD

Design of Experiments/Response Surface Methodology: DoE/RSM

Higher Heating Value: HHV

Hydrothermal carbonization: HTC

Residence time: t

Residence time-Biomass/water ratio: t-R

Solid Yield: SY

Statistical Software Package: SPSS

Temperature: T

Temperature-Biomass/water ratio: T-R

Temperature-Residence time: T-t

1. Introduction

There is an increasing awareness on the unsuitability of current energy consumption scheme, based mainly on the use of fossil fuels. Emissions coming from fossil fuels combustion lead to problems such as global warming, climate change and environmental pollution. Also, fossil fuel reserves are rapidly depleting, while energy consumption is dramatically increasing. As a result, the necessity of renewable and clean energy resources to replace fossil fuels is widely recognized.

Within this frame, there is a growing interest in the development of alternative sources for clean renewable energy production sources such as biomass. Besides, in general terms, biomass does not contribute to global warming since it recycles carbon dioxide from the atmosphere.

The olive oil sector has a significant role in the economy of the European Union. In particular, the EU is the largest world olive oil producer, contributing with 80% of world production, and consumer, 70% of it. EU average production of olive oil in recent seasons was 2.2 million tonnes, of which about 62% corresponded to Spain, making it by far the first Community producer [1]. Olive industry presents a high potential for solid biofuel production because of the residues generated from olive groves and those by olive oil industries. Olive stone is one of the most important residues generated in this sector and could be an interesting renewable energy source. According to González et al (2009) [2] this residue is constituted by cellulose (30.8%), hemicellulose (17.1%) and lignine (32.6%). This lignocellulosic material is mainly used as solid biofuel to thermal power generation [3].

Several forms of pre-treatment can be considered in order to improve the physicochemical characteristics of lignocellulosic biomass for its subsequent combustion. These include drying [4], pelleting [5], ultrasonication [6], washing with chemicals [7], torrefaction [8], etc. In this context, it is interesting to remark that hydrothermal carbonization (HTC) of biomass has gained great relevance during the last few years due to its simplicity and low cost [9,4]. HTC involves heating biomass in water under autogenous conditions, in some cases in the presence of chemicals, to enhance energy densification by yielding a carbonaceous fraction called hydrochar (HC), which is more stable and has higher C content than the raw matter. Previous works in this line have examined the use of biomassic materials such as grass cuttings [10], algae [11], maize [12], invasive aquatic plants [13], and sewage sludge [14]. To the best of the authors' knowledge, no study has considered HTC of the olive stones yet.

Given this context, the objective of the present work was to provide added value to olive stone, a sub-product of the olive oil industry, potentially suitable as a hydrochar precursor. In particular, an HTC process was tested, studying the influence of three processing variables: temperature, residence time, and biomass/water ratio. To gain deeper insight into the HTC process and a more realistic interpretation of the results, a DoE/RSM (Design of Experiments/Response Surface Methodology) approach was used. This is a particularly useful strategy for investigating interactions between variables, which would be hard to verify by a classical 'one variable at a time' approach.

2. Experiments

2.1. Materials

The raw material was olive stone, produced in a company located in Valdetorres (Extremadura, Spain), producing mainly olive oil. After the olive oil extraction, and like a by-product, appear the olive stone mixed with the olive pulp. The olive stone used, was separated from the pulp, and it was grounded and sieved to a particle size of 0.4 - 2.0 mm. Then, the sample was dried overnight at 100 ºC and stored in a closed flask placed in a desiccator until further analysis.

2.2. HTC processes and hydrochar characterization

The HTC processes were performed in a stainless steel autoclave (Berghof, Germany). In a 0.2 L teflon vessel (unstirred), an appropriate amount of sample (5-18.4 g) and 150 mL of deionised water at room temperature were added, in order to obtain the targeted biomass/water ratio, R (1.1-12.3%). Then, the teflon vessel was sealed and placed into the autoclave and the system remained overnight at room temperature. Thereafter, the system was heated up in an electric furnace at selected temperatures (150-250 °C), during a chosen processing time (3.2-36.8 h). When the reaction time was reached, the autoclave was removed from the oven and subsequently placed in a cold-water bath and allowed to cool down up to room temperature. After cooling, solid was separated from liquid by vacuum filtration and subsequently dried at 80 ºC to remove residual moisture. The dried hydrochar was stored in closed flasks placed into a desiccator until further analysis. The experiments were carried out under autogeneous pressure in an autoclave without possibility of measure interior conditions, but according to our studies the pressure inside the vessel corresponds with the water at saturated conditions.

The hydrochars were characterized in terms of their solid yield, higher heating value (HHV, MJ kg^{-1} dry basis), which was determined experimentally by a bomb calorimeter (Parr) [15]. Elemental analysis for carbon, hydrogen, nitrogen, and oxygen were carried out with an elementary analyzer

(Eurovector EA 3000), according to the norm CEN/TS 15104 (for determining the content of C, H and N) and CEN/TS 15289 (for S) (CEN/TS 335 Biomass standards, 2004). The surface chemistry was studied by FTIR spectroscopy. FTIR spectra were recorded with a Perkin Elmer model Paragon 1000PC spectrophotometer, using the KBr disc method, with a resolution of 4 cm^{-1} and 100 scans.

2.3. DoE/RSM procedures

The DoE/RSM approach has proven to be a very useful tool to investigate the influence of several variables on a given magnitude (the output function) [16, 17]. This technique allows the optimal processing conditions to be identified by taking into account the interactions between the different variables involved, unlike the case of classical step-by-step analyses. Moreover, fewer independent runs are required for this optimization.

A Central Composite Design (CCD) is useful in RSM to implement the DoE approach because it provides an even distribution of the experimental points. It involves the use of a two-level factorial design with 2^k points combin ed with 2k axial points and n centre runs, with k being the number of factors. With k factors, the total number of experiments, N, is:

$$N = 2^k + 2k + n \qquad (1)$$

The plot of the CCD for 3 factors is presented in Fig. 1. It can be observed that this experimental design gives a spherical distribution. This homogeneous distribution facilitates the further statistical analysis. **HERE FIGURE 1**

As noted above, the present work involved the analysis of the influence of three variables: temperature (T), residence time (t), and biomass/water ratio (R). Thus the number of factors was k = 3, and, according to Eq. (1) and taking n = 4, the total number of experiments to conduct was 18.

The runs were made randomly in order to avoid hidden effects. A second-order model was used as the equation defining the target function (the response, Y):

$$Y = A_o + A_1R + A_2T + A_3t + A_4RT + A_5Rt + A_6tT + A_7R^2 + A_8T^2 + A_9t^2 \quad (2)$$

Equation (2) was fitted to the experimental results using IBM SPSS statistical software package, and the resulting equations were plotted using Wolfram Mathematica 8 software.

3. Results and Discussion

As was detailed in Sec. 2.3, prior to experimentation, a CCD was used in order to define the experimental conditions to test (operating temperature, residence time, and biomass/water ratio). Based on the results of previous experiments [18], the ranges used for these three parameters were 150–250 °C, 3.2–36.8 h, and 1.1–12.3%, respectively. The values of SY and the corresponding HHVs obtained for each run are listed in Table 1. These results will be discussed in Secs. 3.1 and 3.2, respectively. **HERE TABLE 1**

The Levenberg–Marquardt algorithm was applied to fit the model to the experimental data, using the SPSS software package. The model fits well both SY and HHV data as the high values of R^2 indicate (0.8468 and 0.9031, respectively), thus endowing the further analysis carried out with validity in providing a true picture of the HTC process.

The values of the normalized coefficients (A0 - A9) fitting the target function (Y, eqn. 2), in accordance with the defined model are presented in Table 2.

From this Table the relevance of each variables, as well as their synergies, can be drawn out, as it is described subsequently. **HERE TABLE 2**

3.1. Effect of the variables on the hydrochar yield

From a simple observation of the results presented in Table 1, one can infer that the experimental conditions had a major effect on SY, which ranged between 30.98% and 55.75%.

On the other hand, a preliminary conclusion that can be drawn from the linear normalized coefficients listed in Table 2 (A1-A3) is that increasing both the temperature and the residence time reduce the SY, while a greater R results in higher SY. However, the existence of interactions terms (A4-A6) and quadratics terms (A7-A9) of different sign make difficult to extract a simple conclusion on the effect of each variable. A similar influence of temperature on solids recovery has also been reported in the literature when carbonizing feedstocks such as cellulose, glucose and wood. Lu et al. [19] studied the hydrothermal carbonation of cellulose and suggested that the observed initial decrease in solids recovered results from a combination of initial feedstock solubilization and component partitioning to the gas and liquid-phases, increasing the solid loss with temperature and time. Falco et al. [20] presented two important conclusions from looking at the effect of temperature on the yield in the case of hydrothermally treated glucose: 1) the minimum temperature for the hydrothermal carbon formation from glucose is 160 ºC, below which no measurable quantity of char can be recovered; 2) the maximum yield is achieved at 200 ºC (T range: 120 ºC - 280 ºC), after which it starts to gradually decline. According to the authors, an explanation for this downward trend is that the increase in temperature favors gasification reactions.

In order to gain further insight into the processing variables effect on SY, level curves were plotted (Figs. 3a-i) by fixing in turn each one of the variables to the following values:

R: 3.33%, 6.67%, and 10%

T: 170 °C, 200 °C, and 230 °C

t: 10 h, 20 h, and 30 h.

The nine plots in Figs. 3a-i are the corresponding cutting planes of the spherical domain described by Equation (2) in the R-T-t space. Thus, an analysis of these nine 2D figures will help to understand the behavior of SY in the 3D domain. Some extra graphic elements (arrows, points, lines, etc.) have been added to certain plots in order to facilitate their interpretation.

Figures 2a-c show the T-t level curves corresponding to fixed biomass/water ratios (R = 3.33%, 6.67%, and 10%, respectively). One observes that, in general, for a given T-t condition, an increase in R results in a slight increase in SY. Moreover, in general, the plots show that, the higher the T and t, the lower the SY. However, a more detailed inspection of the level curves reveals that the three plots present different trends. Thus, while at R = 3.33% there is a clear prevalence of the T effect, as R increases the influence of t rises, being t and T effects similar at R = 15%. These facts indicate that although T and t play the main role in the SY, R effect could not be neglected because it affects not only the SY value but also the prominence of T and t as major influencing factor.

Figures 2d-f show the R-t level curves corresponding to fixed temperatures (T = 170 °C, 200 °C, and 230 °C, respectively). Several interesting observations can be made concerning these plots. Firstly, for a given t-R condition, an increase in T results in an important decrease in SY. For example, in T = 170 ºC most of the R-t conditions give rise to SY values higher than 50% while at T = 230 ºC, SY ≥ 50% values are only obtained at short times (<10 h) and high R (>6). On the other hand, as the temperature rises there is a change in the R-t level curve pattern. The importance of t as a controlling factor is only slightly conditioned by T, in the domain studied; at T = 170 ºC the effect of t predominates while at 230 ºC R also plays a main role. The R-t level curve shows an intermediate pattern at T = 200 ºC.

Finally, figures 2g-i show the R-T level curves corresponding to fixed processing times (t = 10 h, 20 h, and 30 h, respectively). Their main features are the following. For a given R-T condition, an increase in t results in a decrease in SY. At short time (t = 10h) a large number of R-T conditions result in SY ≥ 50% while at 20h and 30h SY higher than 50% are obtained only at T lower than 170 ºC and 160 ºC, respectively. Once again, the interactive effects of variables are evidenced; the extent of controlling role of temperature is conditioned by the residence time.

The results show that, in a general view, higher T and t reduces SY while higher R results in slightly higher SY values. However, the detailed effect of the processing variables are rather complex because there is a clear interaction between the three variables and, consequently, the effect of one of these variables depends on the value of the others.

The strong influence of T on the final SY of the HTC reaction is consistent with previous findings in the literature [9, 11, 12, 21]. This has usually been attributed to greater primary decomposition of biomass at high temperatures, or to secondary decomposition of the solid residue. However, there is no such clarity about the effect of residence time. This can be positive, negative, or null, depending on the precursor. For example, He at al. [14] report that longer treatment times increase the SY values due to solid residue formation by re-polymerization of heavy oils. In contrast, our previous work with different precursors found the influence of residence time to be negative or not significant [9]. This variety of results can be explained on the basis of the model described by Knežević et al. who highlight that the formation of hydrochars proceeds by a primary and secondary contribution, the former related to a pyrolysis like mechanisms and the second one to conversion and recombination of secondary products in the bulk [22]. The prominence of these contributions depends on the experimental conditions and that is why the pieces of research found in the bibliography, all step by step analyses made under dissimilar conditions, offer so different results. Using DoE/RSM approach allows acquiring a wider view and to detect these features.

Obviously, since HTC is a very complex process in which a series of simultaneous reactions takes place, such as hydrolysis, dehydration, decarboxylation, aromatization, and re-condensation [19], it is difficult to draw any conclusion on the effect of the process variables by using a classical step-by-step experimental design. A DoE/RSM approach such as used in the present work allows one to analyse the effects of those variables in greater depth, revealing their interactions. This may in part explain the discrepancies in the literature with regard to the influence of the different variables.

3.2. Effect of the variables on the HHV

HHV (defined in Table 1) is also influenced by the processing variables, with the experimental values for HHV ranging from 22.18 to 29.59 MJ kg^{-1}. It is evident, therefore, that varying the experimental conditions allows one to modulate the energy density of the hydrochar over a broad range. The normalized linear coefficients (A1…A3 in Table 2) show the strong influence of T and t on HHV.

Figures 3a-i show the HHV level curves. It is evident that there are important differences with the SY curves.

Figures 3a-c show that, unlike the SY case, the three plots are very similar and there is no change in HHV as R increases. It is evident that T strongly affects the HHV values, with t playing a secondary role. As T rises its influence becomes stronger.

Figures 3d-f show that, as T increases for a given t-R value, HHV also increases, confirming the main role that temperature plays in the process. As T changes, the pattern of the curves remains almost constant, confirming the low interactions among the processing variables. Considering the directions of the gradients, one observes that the effect of t predominates over that of R.

In Figs. 3g-i, it can be seen that the pattern of the T-R level curves has no dependence on the residence time (t). It seems that there is little interdependence of the effects of the processing variables.

It is evident that for the obtained hydrochars from olive stone there is low correlation between HHV and SY (R^2 = 0.4223). On the contrary, we have found a clear linear relationship between HHV and SY (R^2 = 0.8197) in tomato peel hydrochars (data sent to be published).

The above analysis has shown that a DoE/RSM approach provides useful information about the effect of the processing variables on the HTC reaction, and thus can help comprehend this complex process. It can also be a useful tool in selecting the optimal processing conditions to produce hydrochars with certain desired characteristics. To illustrate this possibility, we shall consider in this subsection how the processing conditions can be selected to produce, for example, an hydrochar with an HHV of 28 MJ kg^{-1} from olive stone using a biomass/water ratio equal to 12% while maintaining t ≤ 15 h. Figure 4 shows the temperature-time SY level curves for R = 12%. The experimental constraints (the HHV = 28 MJ kg^{-1} curve and the t = 15 h line) have been drawn onto the graph, so that the shadowed area represent all the pairs T-t that should satisfy this particular demand.

HERE FIGURE 4

3.3. Chemical characteristics of the hydrochar

The elemental composition of some representative hydrochars are shown in Table 3. From these values, and using the atomic ratios, H/C and O/C were calculated. As inferred from this Table, both ratios decrease as a higher temperature is used, in coherence with the enhanced carbonization; previous pieces of research have shown similar results [19].

By FTIR is possible to follow the structural and chemical changes during hydrothermal carbonization. In this study, all the hydrochars showed very similar FTIR spectra no matter the SY reached. From the results obtained it was drawn-out that the surface chemistry of the hydrochars was affected mainly by the effect of temperature, while the remaining variables showed a scant influence. For the sake of brevity, only the FTIR spectra of selected samples (S-10: 6.67% - 150 ºC - 20h, S-15: 6.67% - 200 ºC – 20 h, and S-13: 6.67% - 250 ºC – 20 h, with SY equal to 57.75%, 42.28%, and 39.75%, respectively) have been included in this work, and are plotted in Figure 5. The corresponding peak assignments were made according to the bibliography [23]. From these spectra it can be noticed that using an enhanced temperature results in the shift, appearance or removal of some signals, while some others are maintained. The comparative analysis of these results allows identifying the following groups:

- The absorbance peak around 3440 cm^{-1} is due to the O-H stretching vibration in hydroxyl groups becomes less intense and less symmetric in sample 13, which underwent a greater carbonization. This in turn suggests the prominence of dehydration reactions during hydrocarbonization, in agreement with the elemental analysis.

- The peak at 2920 cm^{-1} indicates the C-H asymmetrical stretching vibration in methyl, methylene and methyne groups, while absorption at 2846 cm^{-1} could be assigned to the symmetrical stretching vibration of these groups. These two signals appear overlapped at 150 ºC (sample 10), while they become separated as temperature is raised.

- The bands at 1730 cm^{-1} and 1630 cm^{-1} are due to C=O stretching vibration of carbonyl groups unconjugated and conjugated with aromatic rings, respectively. These two bands are more intense for the samples made at greater temperature (13 and 15).

- The band at 1515 cm^{-1} can be assigned to the C=C stretching of the aromatic rings, while C-H bending vibration in methyl groups can be assigned to the band of 1460 cm^{-1}. These bands are found in the three samples, indicating that these groups were not affected by temperature.

- The appearance of the C-O stretching bands at 1372 cm^{-1} and 1247 cm^{-1} suggests the existence of syringyl and guaiacyl groups. In this case, the former band was not found for sample 13, while the second one was attenuated for this hydrochar, indicating the sensitivity of these surface groups towards temperature. Similarly, the absorption at 1164 cm^{-1} and 1106 cm^{-1} originates from the C-H deformations in plane of guaiacyl and syringyl units were better defined for the samples made at lower temperature.

- Sample 13 exhibits a band at 985 cm^{-1}, which can be assigned to –C-O stretching in both –C-O-C- in aliphatic ethers and alcohols.

HERE TABLE 4

4. CONCLUSIONS

We have described a study of the hydrothermal carbonization of olive stone residue from industrial olive oil processing, examining the influence of temperature, residence time, and biomass/water ratio. A Central Composite Design method was implemented to define the number and the conditions of the experiments to perform. The resulting experimental data were fitted by a 2nd-order model, allowing the behaviour of the process to be simulated with accuracy.

The following conclusions can be drawn from the results of the study:

1. The application of the DoE/RSM approach to HTC processing of olive stone allowed the construction of models describing SY and HHV as functions of the processing variables (temperature, residence time, and biomass/water ratio). The good fit to the experimental data endows these models with validity to forecast the behaviour of the process for given experimental conditions. The application of this methodological approach showed how complex the HTC process

is in that it identified many interactions among the variables, which would not have been possible using the classical 'one variable at a time' methods. This approach could be a very useful tool for selecting the optimal processing conditions to produce hydrochars with certain desired characteristics.

2. Temperature, T, was undoubtedly the main processing variable affecting the SY of the HTC reaction, followed by the residence time, t, with both causing decreases in SY as they themselves increased. Higher R results only in slightly higher SY values. However, the detailed effect of the processing variables are rather complex because there is a clear interaction between the three variables and, consequently, the effect of one of these variables depends on the value of the others.

3. With respect to energy densification, there was a dependence of HHV on the processing variables, with its experimental values ranging from 22.2 to 29.59 MJ kg^{-1}. Temperature plays the main role in determining the HHV of the resulting hydrochar.

4. There is no clear relationship between HHV and SY.

5. The chemical characteristics of the hydrochars were studied in terms of their elemental composition. Further analysis of the surface functionalities of the hydrochars by FTIR confirmed this effect.

5. ACKNOWLEDGEMENTS

The authors are grateful to "Supporting action plans for Groups registered in the Catalogue of Research Groups of Gobierno de Extremadura”, GR10159.

6. REFERENCES

[1]European Comission 2012. Available at: http://ec.europa.eu/budget/figures/2012/2012_en.cfm

[2] J.F. González, S. Román, J.M. Encinar, G. Martínez, Pyrolysis of various biomass residues and char utilization for the production of activated carbons, J. Anal. Appl. Pyrol, 85 (2009) 134-141.

[3] J. Mata-Sánchez, J.A. Pérez-Jiménez, M.J. Díaz-Villanueva, A. Serrano, N. Núñez-Sánchez, F.J. López-Giménez, Statistical evaluation of quality parameters of olive stone to predict its heating value, Fuel, 113 (2013) 750-756.

[4] H. Song, F. Starfelt, L. Daianova, J. Yan, Influence of drying process on the biomass-based polygeneration system of bioethanol, power and heat, Appl. Energ. 90 (2012) 32-37.

[5] M.T. Miranda, J.I. Arranz, S. Román, S. Rojas, I. Montero, M. López, J.A. Cruz, Characterization of grape pomace and pyrenean oak pellets, Fuel Process. Technol. 92 (2011) 278-283.

[6] A. García, M. González Alriols, J. Labidi, Evaluation of the effect of ultrasound on organosolv black liquor from olive tree pruning residues, Bioresource Technol. 108 (2012) 151-160.

[7] H. Tan, S. Wang, Experimental study of the effect of acid-washing pretreatment on biomass pyrolysis, J. Fuel Chem. Technol. 37 (2009) 668-672.

[8] M.J.C. Van der Stelt, H. Gerhauser, V. Kiel, K.J Ptasinski, Biomass upgrading by torrefaction for the production of biofuels: A review. Biomass Bioenerg., 35 (2011) 3748-3762.

[9] S. Román, J.M.V. Nabais, C. Laginhas, B. Ledesma, J.F. González, Hydrothermal carbonization as an effective way of densifying the energy content of biomass, Fuel Process. Technol. 103 (2012) 78-83.

[10] W. Hao, E. Björjman, M. Lilliestrale, N. Hedin, Activated carbons prepared from hydrothermally carbonized waste biomass used as Adsorbents for CO2, Appl. Energ. 112 (2013) 526–532.

[11] S.M. Heilmann, H.T. Davis, L.R. Jader, P.A. Lefebvre, M.J. Sadowsky, F.J. Schendel, M.G. von Keitz, K.J. Valentas, Hydrothermal carbonization of microalgae, Biomass Bioenerg. 34 (2010) 875-882.

[12] J. Mumme, L. Eckervogt, J. Pielert, M. Diakité, F. Rupp, J. Kern, Hydrothermal carbonization of anaerobically digested maize silage. Bioresource Technol. 102 (2011) 9255-9260.

[13] J.W. Catallo, T.F. Shupe, T.L. Eberhardt, Hydrothermal processing of biomass from invasive aquatic plants, Biomass Bioenerg. 32 (2008) 140-145.

[14] C. He, G. Apostolos, W. Jing-Yuan, Conversion of sewage sludge to clean solid fuel using hydrothermal carbonization: Hydrochar fuel characteristics and combustion behaviour, Appl Energ. 111 (2013) 257-266.

[15] European Committee for Standardization, 2005. Technical Specification CEN/TS 14918: 2005. Solid biofuels-method for the determination of calorific value.

[16] 11.1 D.C. Montgomery, Design and Analysis of Experiments, 5th ed., John Wiley and Sons, (2001) New York.

[17] E. Sabio, F. Zamora, J. Gañan, C.M. González-García, J.F. González, Adsorption of p-nitrophenol on activated carbon fixed-bed, Water Res. 40 (2006) 3053–3060.

[18] S. Román, J.M. Valente Nabais, B. Ledesma, J.F. González, C. Laginhas, M.M. Titirici, Production of low-cost adsorbents with tunable surface chemistry by conjunction of hydrothermal carbonization and activation processes, Micropor. Mesopor. Mat. 165 (2013) 127-133.

[19] X. Lu, P.J. Pellechia, J.R.V. Flora, N.D. Berge, Influence of reaction time and temperature on product formation and characteristics associated with the hydrothermal carbonization of cellulose, Bioresource Technol. 138 (2013) 180–190.

[20] C. Falco, N. Baccile, M.M. Titirici, Morphological and structural differences between glucose, cellulose and lignocellulosic biomass derived hydrothermal carbons, Green Chem. 13 (2011) 3272-3281.

[21] G.K. Parshetti, Z. Liu, A. Jain, M.P. Srinivasan, R. Balasubramanian, Hydrothermal carbonization of sewage sludge for energy production with coal, Fuel 111 (2013) 201-210.

[22] D. Knežević, W.van Swaaij, S. Kersten, Hydrothermal Conversion Of Biomass. II. Conversion Of Wood, Pyrolysis Oil, And Glucose In Hot Compressed Water, Ind. Eng. Chem. Res. 49 (2010) 104–112.

[23] P.E. Fanning, M.A. Vannice. A drifts study of the formation of surface groups on carbon by oxidation. Carbon 31 (1993) 721–730.

TABLES

Table 1. Obtained values for the different samples of the HC, moving Ratio, Temperature and Residence Time. With the target values of SY and HHV.

Sample	R (%)	Temperature (°C)	Time (h)	SY (%)	HHV (MJ kg^{-1})
1	3.33	170	10	49.47	22.2
2	10.00	170	10	55.49	22.88
3	3.33	230	10	33.21	28.43
4	3.33	170	30	50.62	23.34
5	10.00	230	10	43.22	28.21
6	10.00	170	30	44.3	23.35
7	3.33	230	30	30.98	28.71
8	10.00	230	30	46.82	29.59
9	1.06	200	20	34.68	23.75
10	6.67	150	20	57.75	22.18
11	6.67	200	3.2	63.35	21.44
12	12.27	200	20	47.43	25.65
13	6.67	250	20	39.75	30.83
14	6.67	200	36.8	42.19	28.37
15	6.67	200	20	42.28	26.11
16	6.67	200	20	45.52	24.9
17	6.67	200	20	42.57	27.15
18	6.67	200	20	43.46	26.83

Table 2. Normalized Coefficients A0-A9, R^2 and Standard error (SE) values obtained in the function Solid Yield and High Heating Value.

Coefficients		**Solid Yield**	**Standard error Solid Yield**	**Higher Heating Value**	**Standard error Higher Heating Value**
	A0	43.634	2.359	26.223	0.664
R	A1	3.442	1.279	0.333	0.360
T	A2	-5.562	1.279	2.790	0.360
t	A3	-3.241	1.279	1.093	0.360
RT	A4	3.269	1.671	-0.003	0.471
Rt	A5	-0.814	1.671	0.055	0.471
Tt	A6	1.426	1.671	0.005	0.471
R^2	A7	-1.616	1.331	-0.442	0.375
T^2	A8	1.110	1.331	0.235	0.375
t^2	A9	2.535	1.331	-0.371	0.375
R^2		0.8468		0.9031	

Table 3: Elemental analysis and H/C and O/C atomic ratios for selected hydrochars (samples 10, 13 and 15).

Sample	N (%)	C (%)	H (%)	S (%)	O[a] (%)	Molecular[b] formula	H/C	O/C
10	0.06	54.79	5.83	-	39.32	$CH_{1,27}O_{0,54}$	1.27	0.54
13	0.18	72.03	4.7	-	23.09	$CH_{0,98}O_{0,38}$	0.78	0.24
15	0.07	63.05	5.18	-	31.7	$CH_{0,78}O_{0,24}$	0.98	0.38

[a] Balanced; [b]N and S are discarded due to their low value.

Table 4. Main bands and corresponding assignments.

Num	Vibration (cm^{-1})	Assignments
1	3440	O-H stretching
2	2920	C-H_x unsymmetrical stretching
3	2846	C-H_x symmetrical stretching
4	1730	C=O stretching unconjugated to aromatic ring
5	1630	C=O stretching conjugated to aromatic ring
6	1515	Aromatic ring vibrations
7	1460	C-H bending vibration in methyl groups
8	1372	C-O stretch in syringyl rings
9	1247	C-O stretch in guaiacol rings
10	1164	C-H in plane deformations of guaiacyl units
11	1106	C-H in plane deformations of syringyl units
12	985	C-O deformation in primary alcohols or aliphatic ethers plus aromatic C-H deformation

FIGURE CAPTIONS

Figure 1. Representation of the CCD points for 3 factors

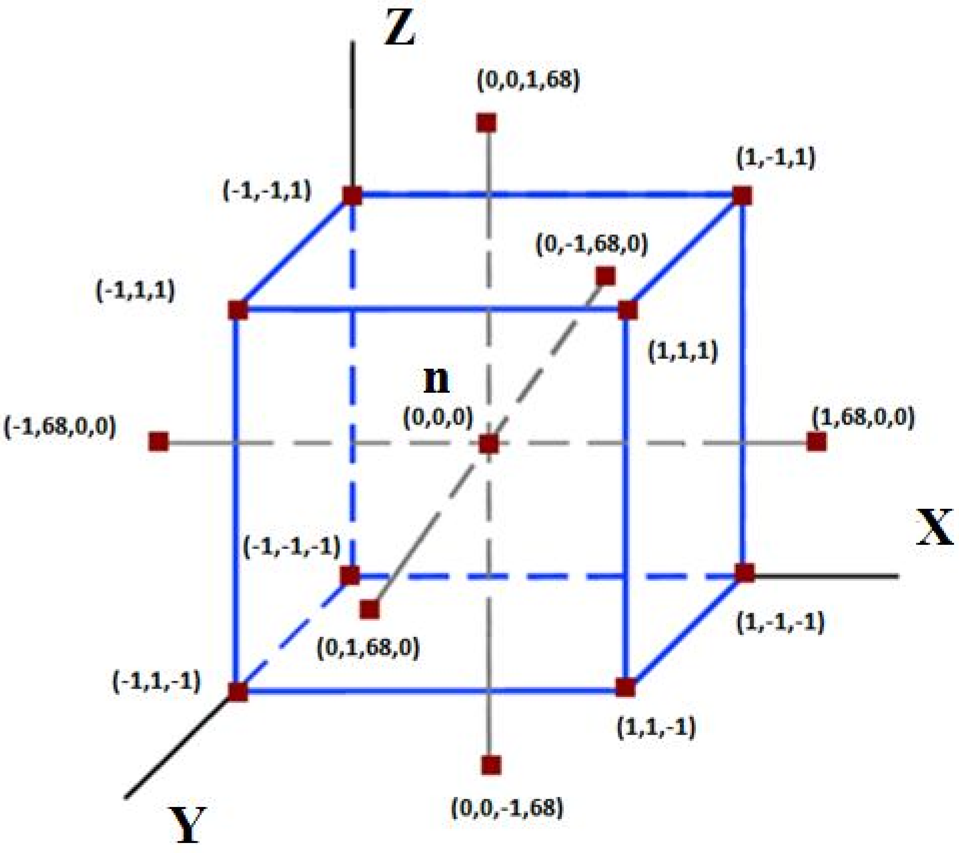

Figure 2. Solid yield of the HC. a-c): R = 3.33 – 6.67 – 10%. d-f): T=170 – 200 – 230 ºC. g-i): t = 10 – 20 – 30 h.

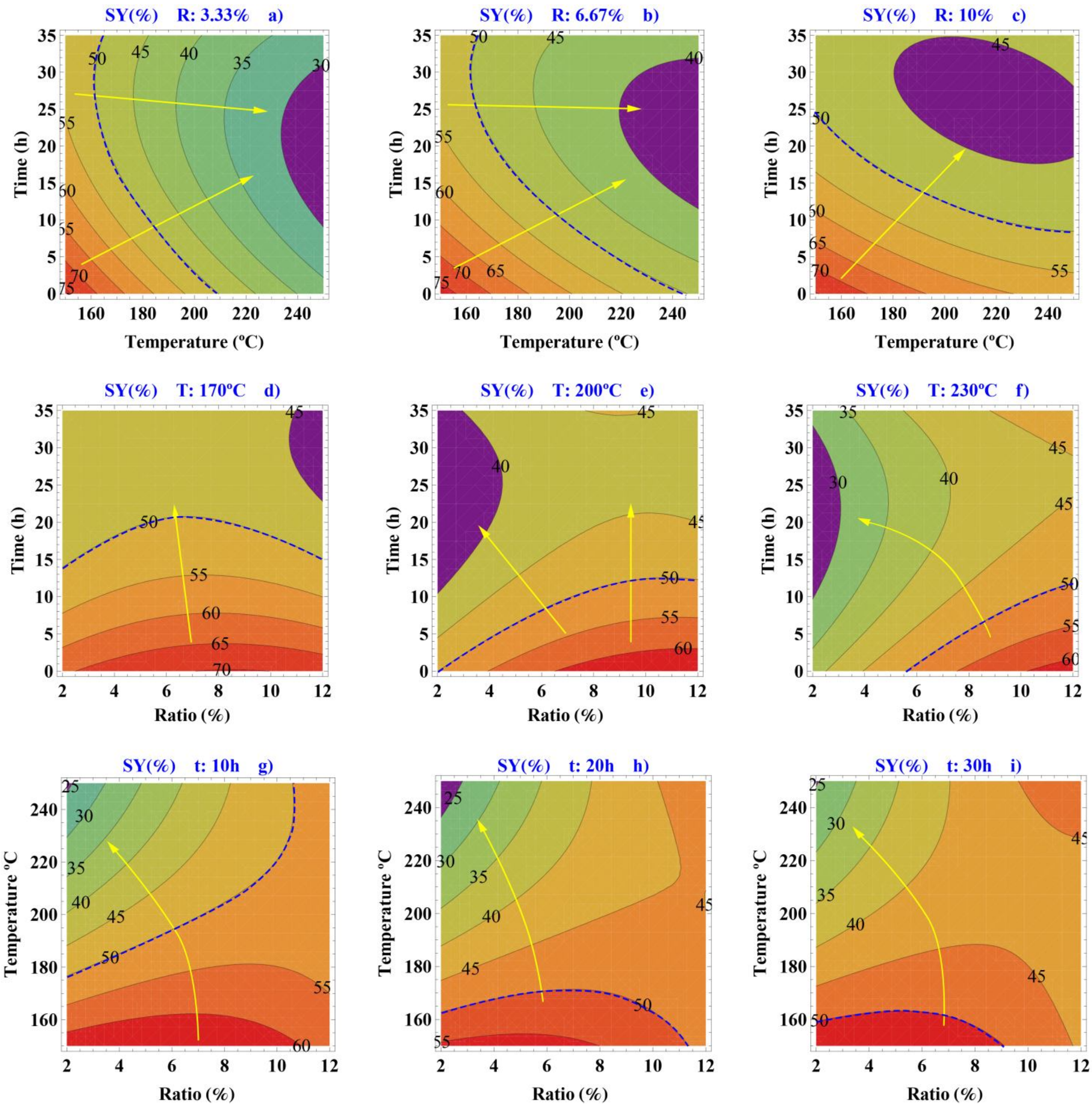
SY(%) R: 3.33% a)
SY(%) R: 6.67% b)
SY(%) R: 10% c)
SY(%) T: 170ºC d)
SY(%) T: 200ºC e)
SY(%) T: 230ºC f)
SY(%) t: 10h g)
SY(%) t: 20h h)
SY(%) t: 30h i)
Time (h)
Temperature (ºC)
Ratio (%)
Temperature ºC
0
5
10
15
20
25
30
35
160
180
200
220
240
2
4
6
8
10
12
25
30
35
40
45
50
55
60
65
70
75

Figure 3. HHV of the HC. a-c): R = 3.33 – 6.67 – 10%. d-f): T = 170 – 200 – 230ºC. g-i): t = 10 – 20 – 30 h.

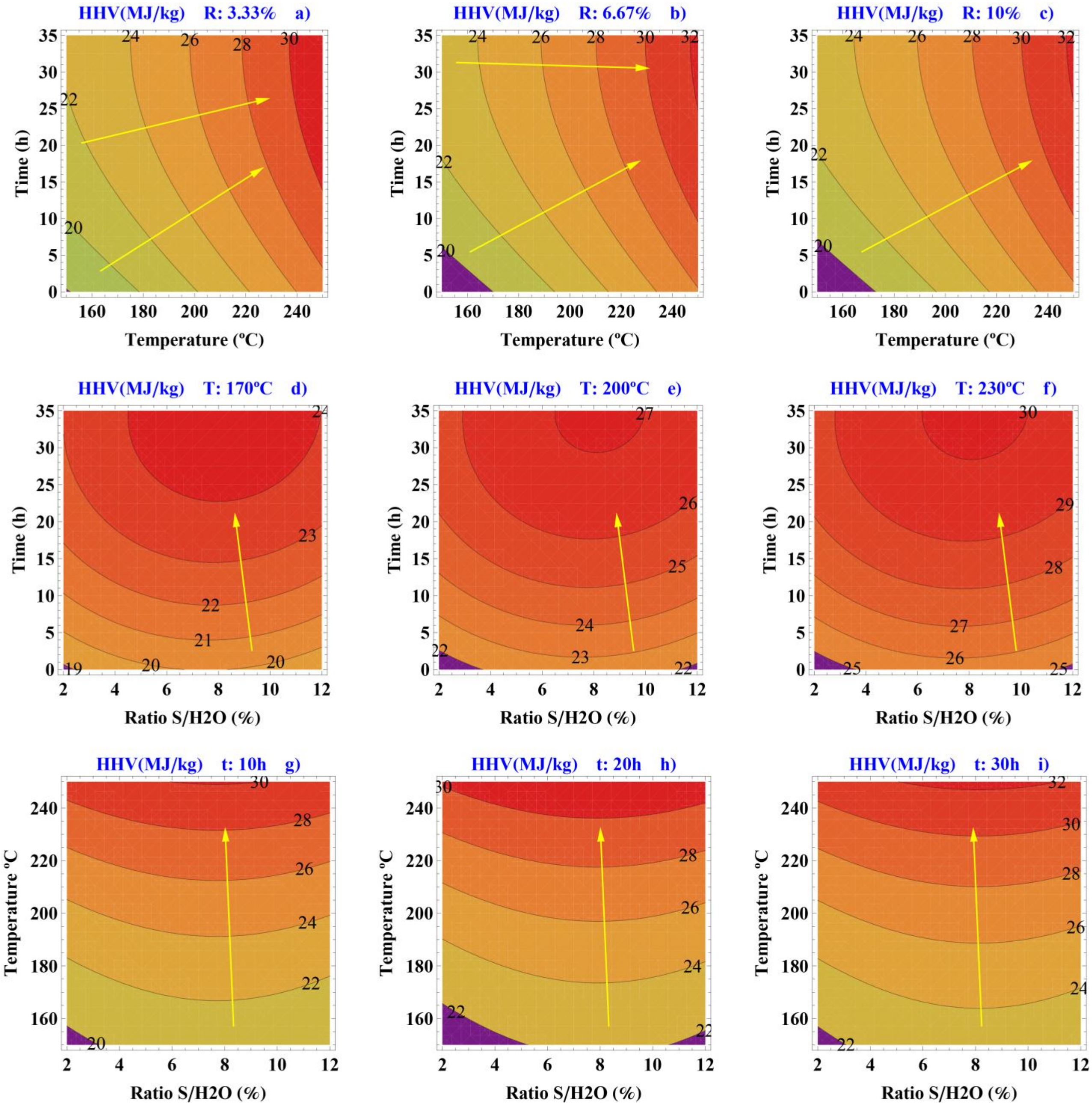

Figure 4. Temperature – time intersection of SY and HHV of R = 12%.

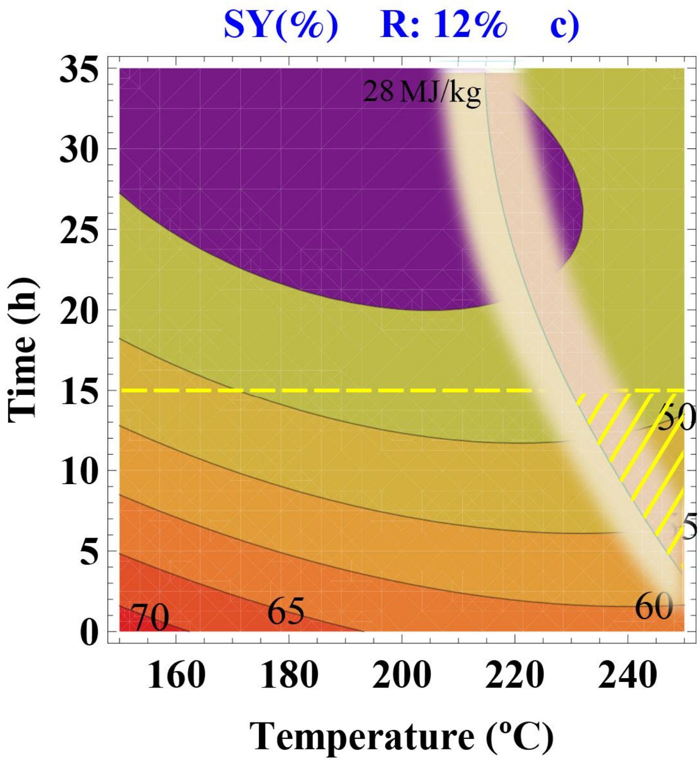

Figure 5. FTIR spectra of samples (10, 13 and 15).

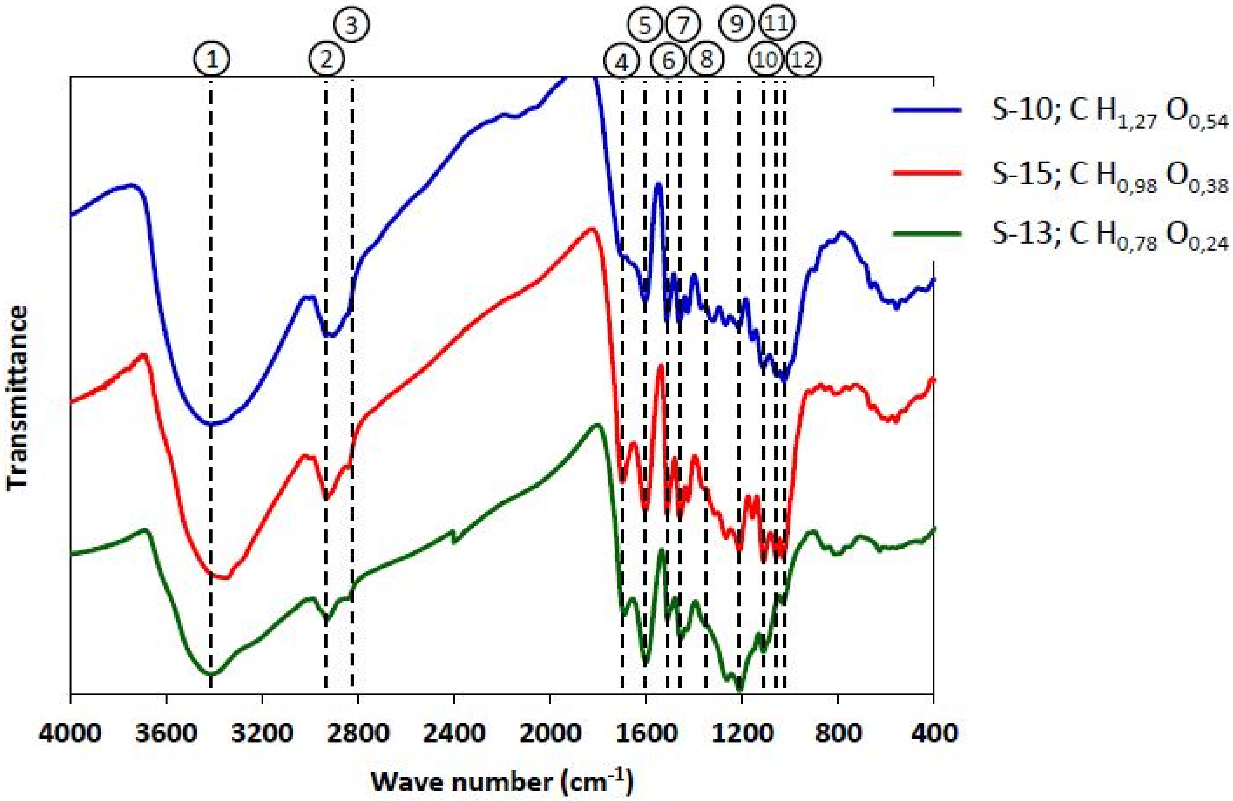
①
②
③
④
⑤
⑥
⑦
⑧
⑨
⑩
⑪
⑫
S-10; C $H_{1,27}$ $O_{0,54}$
S-15; C $H_{0,98}$ $O_{0,38}$
S-13; C $H_{0,78}$ $O_{0,24}$
Transmittance
4000
3600
3200
2800
2400
2000
1600
1200
800
400
Wave number (cm^{-1})